CIRRELT

Centre interuniversitaire de recherche
sur les réseaux d'entreprise, la logistique et le transport

Interuniversity Research Centre
on Enterprise Networks, Logistics and Transportation

An Aggregation Method for Performance Evaluation of a Tandem Homogenous Production Line with Machines Having Multiple Failure Modes

Ahmed-Tidjani Belmansour
Mustapha Nourelfath

November 2008

CIRRELT-2008-53

Bureaux de Montréal :
Université de Montréal
C.P. 6128, succ. Centre-ville
Montréal (Québec)
Canada H3C 3J7
Téléphone : 514 343-7575
Télécopie : 514 343-7121

Bureaux de Québec :
Université Laval
Pavillon Palasis-Prince, local 2642
Québec (Québec)
Canada G1K 7P4
Téléphone : 418 656-2073
Télécopie : 418 656-2624

www.cirrelt.ca

An Aggregation Method for Performance Evaluation of a Tandem Homogenous Production Line with Machines Having Multiple Failure Modes

Ahmed-Tidjani Belmansour[1], Mustapha Nourelfath[1,*]

[1] Interuniversity Research Centre on Enterprise Networks, Logistics and Transportation (CIRRELT) and Département de génie mécanique, Pavillon Adrien-Pouliot, Université Laval, Québec, Canada G1K 7P4

Abstract. This paper presents an analytical aggregation method for evaluating the throughput (or production rate) of tandem homogenous production lines. Unlike in existing aggregation methods, each machine can have more than one failure mode. The flow of processed parts is considered as a continuous flow of material. The aggregation algorithm consists in recurrent replacing of a dipole by a single machine. This replacement is based on five steps: (*i*) construction of a Markov chain (MC) representing a dipole where the machines have multiple failure modes; (*ii*) evaluation of the state probabilities by solving balance equations; (*iii*) classification of MC states into macro-states; (*iv*) evaluation of the transition rates between the macro-states; (*v*) estimation of the production rate of the dipole while taking into account the environment of the aggregated dipole. To assess the accuracy of the proposed method, simulation and numerical experiments have been conducted. A comparison is made between our method and existing aggregation techniques that consider only one failure mode. It is shown that by distinguishing among different failure modes, a more accurate throughput evaluation is obtained.

Keywords. Production lines, buffers, multiple failure modes, throughput evaluation, aggregation, Markov chains.

Acknowledgements. The authors would like to thank the Natural Sciences and Engineering Research Council of Canada (NSERC) for financial support.

---

* Corresponding author: Mustapha.Nourelfath@cirrelt.ca

Dépôt légal – Bibliothèque et Archives nationales du Québec,
Bibliothèque et Archives Canada, 2008

1. Introduction

In production lines, machines can be subject to different kinds of failures which occur with different frequencies and require different amounts of time to be repaired. This paper presents an analytical method for the performance evaluation of a tandem production line (see Figure 1), where the parts are moved from one machine to the next by some kind of transfer mechanism. Each machine is subject to one or many failure modes. The machines are separated by finite capacity buffers. The parts are stocked in these buffers when downstream machines are down or busy.

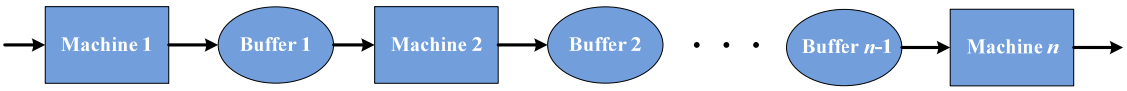

Figure 1. Tandem production line.

A number of methods have been developed for analyzing tandem production lines (also called transfer lines). See for example (Dallery and Gershwin, 1992) or (Papadopoulos and Heavey, 1996) for a survey and a list of references. The performance of a tandem production line is usually measured in terms of production rate (or throughput), *i.e.* the steady state average number of parts produced per time unit. This production rate is in general difficult to evaluate exactly by analytical Markov models. This difficulty is mainly due to exponential growth of the number of states. As a result, most of the methods used to analyze long lines are based either on analytical approximation methods or simulation. Simulation models are applicable to a wide class of systems, but are more expensive computationally (Sörensen and Janssens, 2004). Analytical approximation methods are generally based on the Markov model developed for a line with two machines and one buffer (Dubois and Forestier, 1982) and either aggregation approach (De Koster, 1987; Terracol and David, 1987(a), (b)) or decomposition approach (Gershwin, 1987; Dallery *et al.,* 1989; Tolio *et al.,* 2002; Levantesi *et al.,* 2003; Li, 2005).

In this paper, we develop an aggregation method to evaluate the production rate of a tandem production line where the machines can be subject to multiple failure modes. Existing aggregation techniques are not able to properly deal with more than one failure mode. Therefore, each machine failure mode must be approximated into one average failure. This approximation may cause an error which is not negligible, especially when the reliability parameters (average failure time and average repair time) of

different failure modes have different order of magnitudes (Levantesi *et al.*, 2002; Belmansour, 2007). The proposed method is able to deal with such situations adequately. To assess the accuracy of this method, simulation and numerical experiments have been performed. This aggregation method is sufficiently rapid for evaluation of alternatives within combinatorial optimization algorithms such as those developed in (Nourelfath *et al.,* 2005; Nahas *et al.,* 2006; Nahas *et al.,* 2008).

The remainder of this paper is organized as follows. Section 2 presents the assumptions and the notations. Section 3 outlines the aggregation method proposed to evaluate the production rate of tandem production lines with multiple failure modes. The detailed description of this method is given in Section 4. Simulation results and numerical experiments are reported in Section 5. Finally conclusions are given in Section 6.

2. Assumptions and notations

We consider a tandem production line as shown in Figure 1. The machines are denoted by $M_1, M_2,\ldots, M_n$ and the intermediate buffers by $B_1, B_2,\ldots, B_{n\text{-}1}$. Parts flow from outside the system to machine M_1, then to buffer B_1, then to machine M_2 and so forth until they reach machine M_n, after which they leave the system. It is assumed that the flow of processed parts resembles a continuous fluid. A buffer capacity separating adjacent machines M_j and M_{j+1} (with $j = 1, 2,\ldots, n\text{-}1$) is denoted by N_j. A machine is *starved* if its upstream buffer is empty. It is called *blocked* if its downstream buffer is full. Indeed, the production rate of the tandem production line may be improved by the buffers, as they may prevent blocking and/or starvation of machines. As it is usually the case for production systems, we assume that the failures are operation-dependent, *i.e.* a machine can fail only while it is processing parts (it is said to be working). Thus, if a machine is operational (*i.e.* not down) but starved or blocked, it cannot fail.

Each machine M_j can fail in R_j different modes. We assume that all times to failure and times to repair are exponentially distributed. Let $MTBF_{ij}$ denote the *Mean Time Between Failures* of machine M_j in mode i (with $i = 1, 2,\ldots, R_j$), then $\lambda_{ij} = \frac{1}{MTBF_{ij}}$ is its corresponding failure rate. Similarly, $MTTR_{ij}$ and $\mu_{ij} = \frac{1}{MTTR_{ij}}$ are the *Mean Time To Repair* and the repair rate of M_j in mode i.

We assume that the processing time of each machine is deterministic, *i.e.* a fixed amount of time is required to perform the operation. Thus, machine M_j has a constant cycle time θ_j and a nominal production

rate $U_j = \frac{1}{\theta_j}$. The nominal rate U_j represents the maximum rate at which the machine M_j can operate when it is not slowed down by an upstream or a downstream machine (Gershwin, 1994). It is assumed that the considered line is homogenous, which means that all machines have the same processing time. That is, $U_1 = U_2 = \ldots = U$.

The following additional assumptions are also used:

- the first machine is never starved, *i.e.* there is always available part at the input of the line;
- the last machine is never blocked, *i.e.* finished parts leave the machine M_n immediately or there is always available space for part storage at the output of the line;
- a working machine can fail in only one of its failure modes. Once it is down in a certain mode, it cannot experience a different mode before being repaired;
- the machines have the same number of failure modes ($R_1 = R_2 = \ldots = R$);
- there exists a stationary regime where a steady-state behaviour is reached.

3. Outline of the proposed aggregation method

All the existing aggregation methods deal with tandem production lines with single failure machines (De Koster, 1987; Terracol and David, 1987(a), (b)). The common principle of these methods is to consider a dipole configuration (*i.e.* two adjacent machines and one buffer) as behaving as a single machine, and then to reduce iteratively the number of machines until obtaining only one machine. This aggregation principle is sketched in Figure 2 for a tandem production line with four machines. Such a principle will be used to develop our method for production rate evaluation of tandem production lines with multiple failure modes.

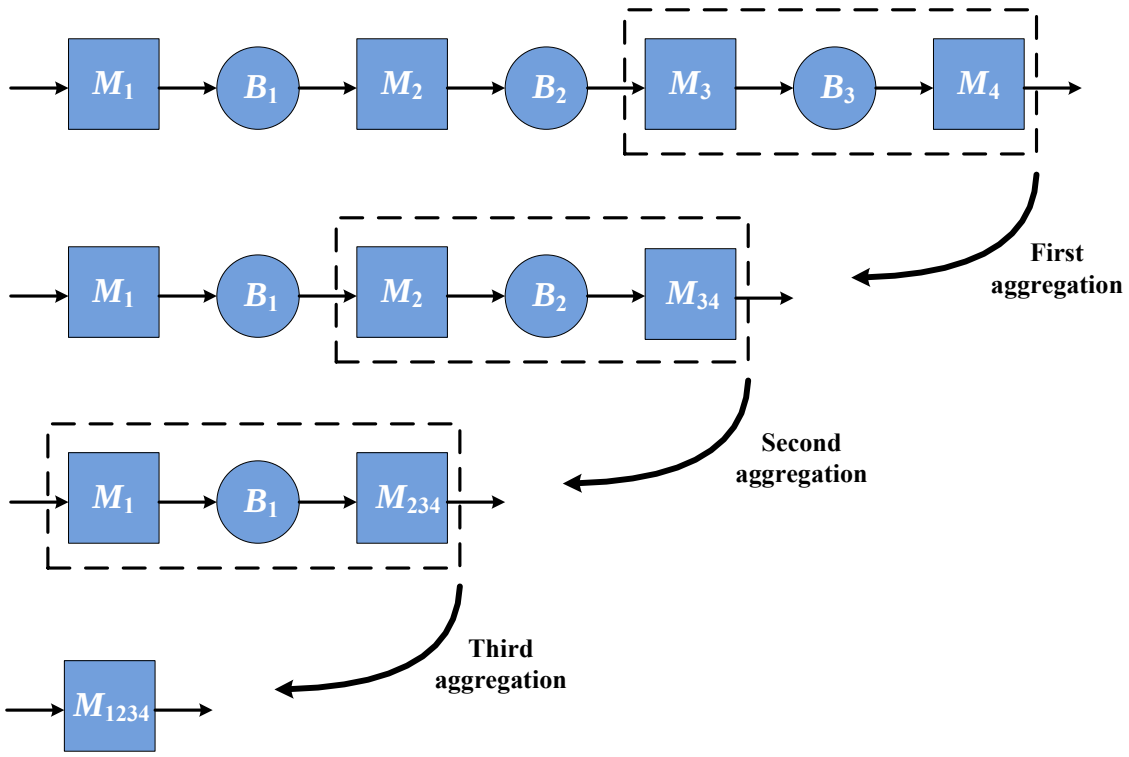

Figure 2. Illustration of the aggregation principle.

The aggregation algorithm for production rate evaluation consists in recurrent replacing of a dipole by a single machine. Therefore, the main step of our method is to replace a dipole, *i.e.* two machines with multiple failure modes and one buffer, by an equivalent machine. The method proposed for this replacement is based on the following steps:

(*i*) construction of a Markov chain (MC) representing a dipole where the machines have multiple failure modes;

(*ii*) evaluation of the state probabilities by solving Chapman-Kolmogorov (or balance) equations for MC;

(*iii*) classification of MC states into a set of working states and multiple sets of down (or failure) states. The set of working states are then grouped to form a macro-state representing the working state of the equivalent machine (M_{eq}). To each set of down states will also correspond a macro-state representing a failure mode state of M_{eq};

(*iv*) evaluation of the transition rates between the different macro-states of M_{eq}. These transitions correspond to the reliability parameters of M_{eq}, *i.e.* its failure and repair rates;

(*v*) estimation of the production rate of the dipole.

Each one of the above five steps are now detailed by considering the following cases:

Case 1- Each machine has two failure modes. This case is denoted by (2, 2);

Case 2- Machines M_j and M_{j+1} have the same number of failure modes ($R_j = R_{j+1} = R$). This case is denoted by (R, R).

Case (R, R) contains case (2, 2). However, we will sometimes develop case (2, 2) before case (R, R): we believe this should help the reader to follow our developments more easily.

4. Detailed description of the method

4.1. Construction of the dipole Markov chain

4.1.1. Each machine has two failure modes

Considering a dipole configuration composed of M_j, B_j and M_{j+1} (Figure 3), we have that $U_j = U_{j+1} = U$ (*i.e.* homogenous dipole). Each machine M_k ($k = j$, j+1) is characterized by a quintuplet (U, λ_{1k}, μ_{1k}, λ_{2k}, μ_{2k}). The dynamics of each machine M_k is described by a continuous-time, discrete-state Markov chain (see Figure 4). Initially, M_k is in its working state W_k and it produces with a nominal rate U. This machine can reach a down state (where the production rate is 0) either by failure mode 1 (state D_{1k}) or by failure mode 2 (state D_{2k}).

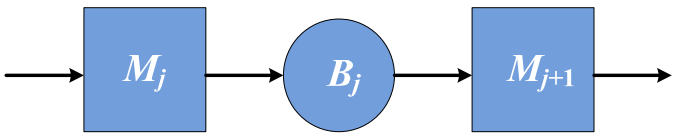

Figure 3. Dipole configuration.

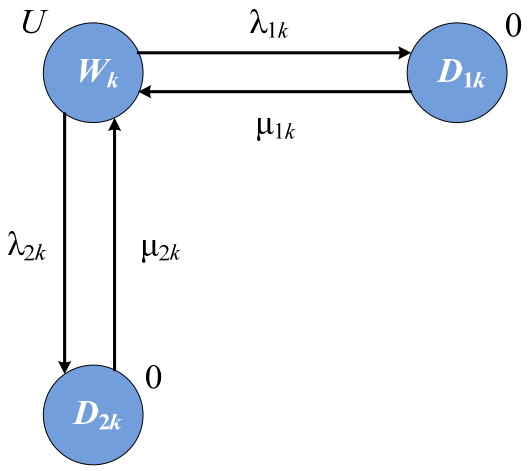

Figure 4. Markov chain of a machine M_k with two failure modes.

The state of the continuous flow system (*i.e.* M_j, B_j and M_{j+1}) is represented by a vector $(x, \alpha_j, \alpha_{j+1})$ where x is the buffer level $(0 \le x \le N_j)$, and $\alpha_k \in \{W_k, D_{1k}, D_{2k}\}$, $k = j, j+1$. That is, α_j and α_{j+1} are the states of machines M_j and M_{j+1}, respectively.

The stochastic process representing the system contains both continuous and discrete states, since the state space is $S = [0, N_j] \times \{W_k, D_{1k}, D_{2k}\}^2$. Two kinds of states are considered:

- the internal states $S_i =]0, N_j[\times \{W_k, D_{1k}, D_{2k}\}^2$; and
- the boundary states $S_b = (\{N_j\} \times \{W_k, D_{1k}, D_{2k}\}^2) \cup (\{0\} \times \{W_k, D_{1k}, D_{2k}\}^2) = S_H \cup S_L$, where S_H is the set of high boundary states $(x = N_j)$ and S_L is the set of low boundary states $(x = 0)$.

There are 9 reachable internal states $(x, \alpha_j, \alpha_{j+1})$. Figure 5 defines the state transition diagram, also called stochastic automaton in this paper, of machines M_j and M_{j+1} when the buffer level is $x \in]0, N_j[$.

The stochastic automaton of Figure 5 corresponds to the composition (Hopcroft and Ullman, 1979) of the stochastic automata of M_j and M_{j+1} given by Figure 4. As this automaton results from the composition of 2 automata of 3 states each, its number of states is $3^2 = 9$. All these states are reachable and they are the elements of the set S_i defined above (*i.e.* the set of internal states). Without loss of generality, to make the notations easier, we will consider sometimes that $j = 1$. This is the case in Figure 5 and Tables 1 and 2 as well.

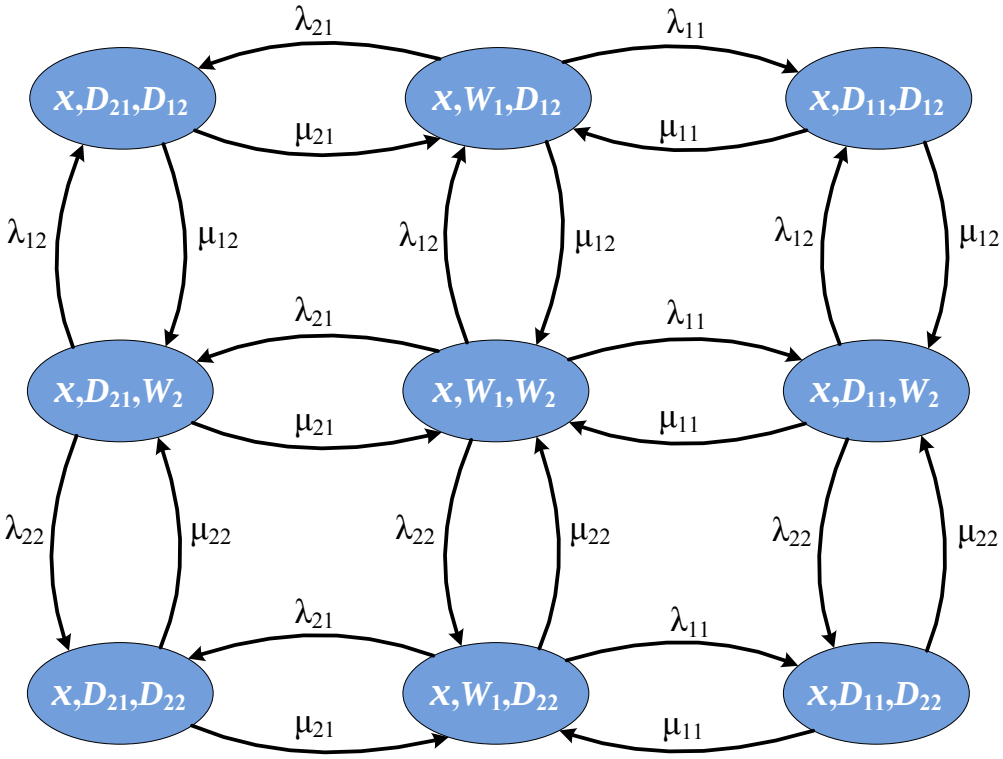

Figure 5. State transition diagram when x ∈ $]0, N_j[$ for case (2, 2).

Tables 1 and 2 present the other combinations of states. There are 9 possible states of the form $(N_j, \alpha_j, \alpha_{j+1})$ and 9 others with the form $(0, \alpha_j, \alpha_{j+1})$. However, many of these states are not reachable. In Tables 1 and 2, we indicate with justification if a given combination leads to a reachable state or not. In these Tables, the state of an operational machine that is starved is denoted by $\underline{W_k}$, while the state of an operational machine that is blocked is denoted by $\overline{W_k}$.

Table 1. Combinations of states when the buffer is full for case (2, 2).

Reference	State	Justification
H1	(N_1, D_{11}, W_2)	Unreachable: as M_2 is working and M_1 is down, the buffer will necessarily decrease.
H2	(N_1, D_{11}, D_{21})	Unreachable: see remark 1 below.
H3	(N_1, D_{11}, D_{22})	Unreachable: similar to state H2.
H4	(N_1, D_{12}, W_2)	Unreachable: similar to state H1.
H5	(N_1, D_{12}, D_{21})	Unreachable: similar to state H2.
H6	(N_1, D_{12}, D_{22})	Unreachable: similar to state H2.
H7	$\left(N_1, \overline{W_1}, D_{21}\right)$	Reachable: when M_1 is working and M_2 is down, the buffer will become full; then, M_1 becomes blocked.
H8	$\left(N_1, \overline{W_1}, D_{22}\right)$	Reachable: similar to state H7.
H9	(N_1, W_1, W_2)	Reachable: when M_2 is repaired from state H7 or H8, this state is reached knowing that $U_1 = U_2$.

Remark 1.

State (N_1, D_{11}, D_{12}) is unreachable because the only way to reach it is either to transit:

- from state (N_1, D_{11}, W_2) which is unreachable; or
- from state $\left(N_1, \overline{W_1}, D_{12}\right)$; but since M_1 is blocked, it cannot fail and such a transition is not possible.

Table 2. Combinations of states when the buffer is empty for case (2, 2).

Reference	State	Justification
L1	$\left(0, D_{11}, \underline{W_2}\right)$	Reachable: when M_1 is down and M_2 is working, the buffer will be empty; then M_2 becomes starved.
L2	$(0, D_{11}, D_{12})$	Unreachable: see remark 2 below.
L3	$(0, D_{11}, D_{22})$	Unreachable: similar to state L2.
L4	$\left(0, D_{21}, \underline{W_2}\right)$	Reachable: similar to state L1.
L5	$(0, D_{21}, D_{12})$	Unreachable: similar to state L2.
L6	$(0, D_{21}, D_{22})$	Unreachable: similar to state L2.
L7	$(0, W_1, W_2)$	Reachable: when M_1 is repaired from state L1 or L4, this state is reached knowing that $U_1 = U_2$.
L8	$(0, W_1, D_{12})$	Unreachable: as M_1 is working and M_2 is down, the buffer cannot be empty.
L9	$(0, W_1, D_{22})$	Unreachable: similar to state L8.

Remark 2.

State $(0, D_{11}, D_{12})$ is unreachable because the only way to reach it is either to transit:

- from state $(0, W_1, D_{12})$ which is unreachable; or
- from state $\left(0, D_{11}, \underline{W_2}\right)$; but since M_2 is starved, it cannot fail and such a transition is impossible.

As the reachable boundary states are now identified, we have to find the remaining feasible transitions for the dipole Markov chain. For this, we consider each boundary state and we determine all feasible transitions from and to this state.

High boundary states

- From state (N_1, W_1, W_2), The transitions that are physically possible corresponds to $\lambda_{11}, \lambda_{21}, \lambda_{12}$ and λ_{22}. At the occurrence of λ_{11} or λ_{21} (failure of M_1), the buffer level will decrease to reach (x, D_{11}, W_2) or (x, D_{21}, W_2), respectively. At the occurrence of λ_{12} or λ_{22} (failure of M_2), the buffer remains full and the reached state is $(N_1, \overline{W_1}, D_{12})$ or $(N_1, \overline{W_1}, D_{22})$, respectively.

- From states $(N_1, \overline{W_1}, D_{12})$ and $(N_1, \overline{W_1}, D_{22})$, the only feasible transitions are μ_{12} and μ_{22}, respectively.

Figure 6 illustrates the partial graph obtained for the high boundary states described above.

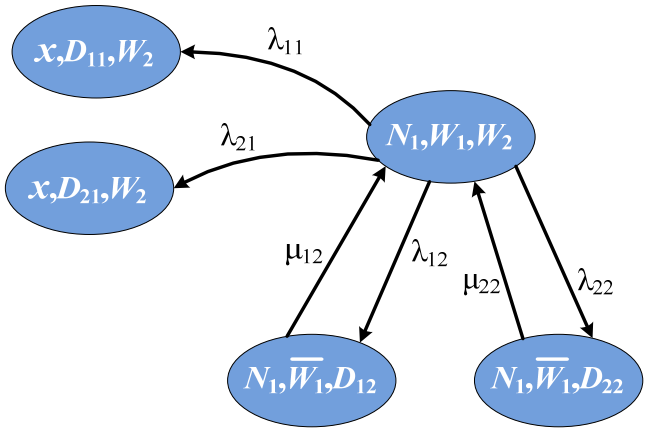

Figure 6. Partial graph for high boundary states.

Low boundary states

- From state $(0, W_1, W_2)$, the transitions that are physically possible are $\lambda_{11}, \lambda_{21}, \lambda_{12}$ and λ_{22}. At the occurrence of λ_{11} or λ_{21} (failure of M_1), the buffer remains empty while M_2 is starved, and the reached state is $(0, D_{11}, \underline{W_2})$ or $(0, D_{21}, \underline{W_2})$, respectively. At the occurrence of λ_{12} or λ_{22} (failure of M_2), the buffer level will increase to reach (x, W_1, D_{12}) or (x, W_1, D_{22}), respectively.

- From state $(0, D_{11}, \underline{W_2})$ and $(0, D_{21}, \underline{W_2})$, the only feasible transitions are μ_{11} and μ_{21}, respectively.

Figure 7 illustrates the partial graph obtained for the low boundary states.

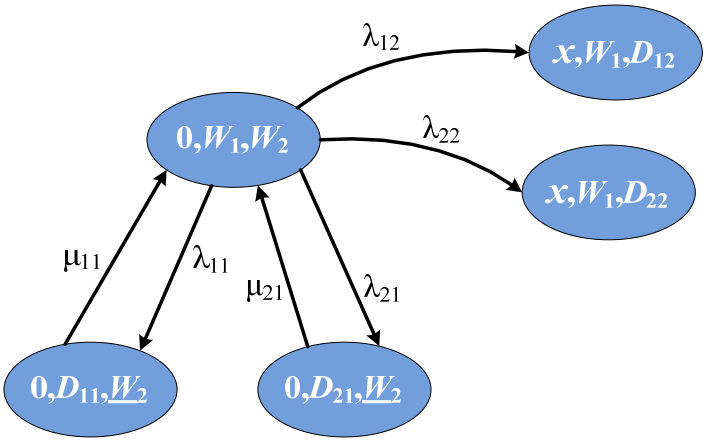

Figure 7. Partial graph for low boundary states.

Finally, by merging Figures 5-7, we obtain directly the dipole Markov chain (MC) sketched in Figure 8.

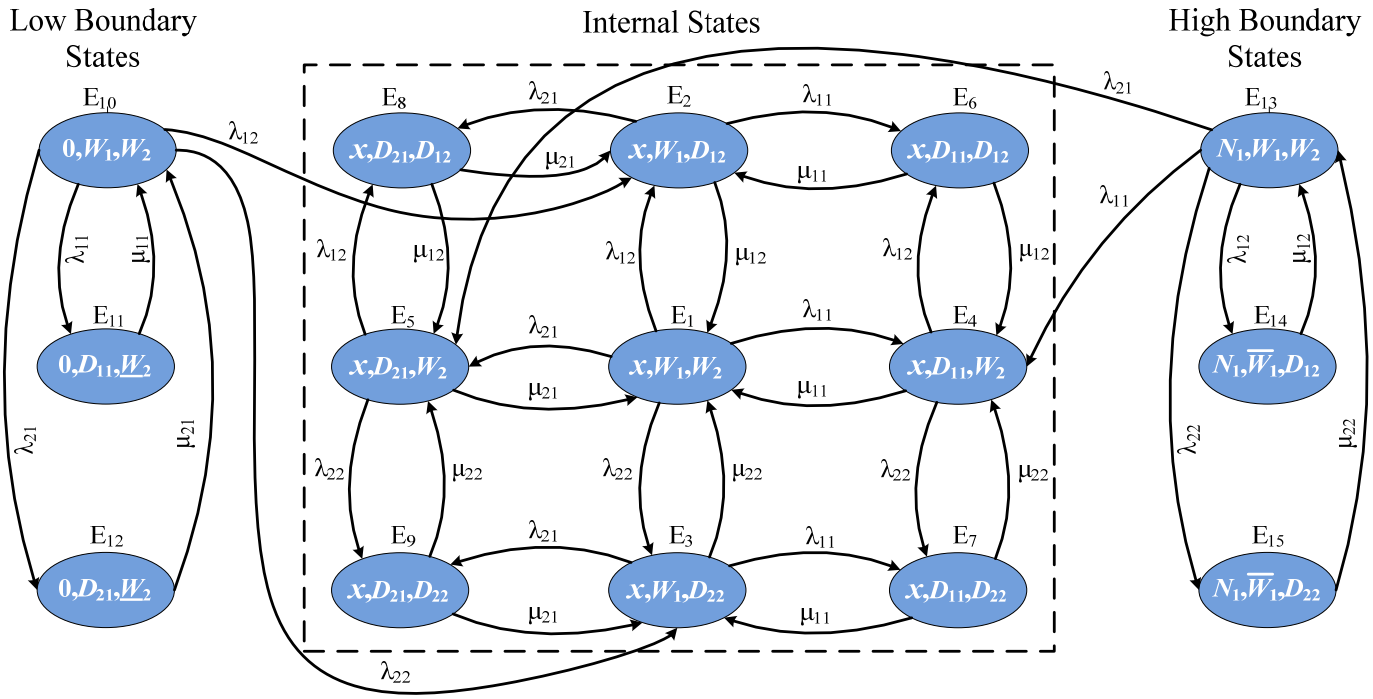

Figure 8. The dipole Markov chain for case (2, 2).

4.1.2. Each machine has *R* failure modes

Let us now generalize our procedure to construct the dipole Markov chain in the presence of more than 2 failure modes (*i.e.* for case (R, R)). The Markov chain describing the dynamics of a machine M_k with R failure modes is given in figure 9.

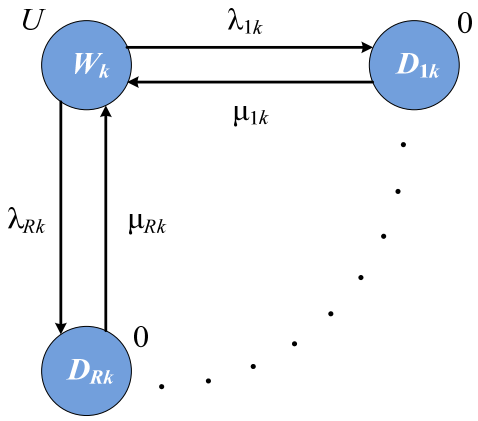

Figure 9. Markov chain of a machine M_k with R failure modes.

Following the same approach as for case (2, 2), Figure 10 defines the state transition diagram when the buffer level is $x \in]0, N_j[$. This diagram contains all internal states and corresponds to the composition of the stochastic automata M_j and M_{j+1} given by Figure 9.

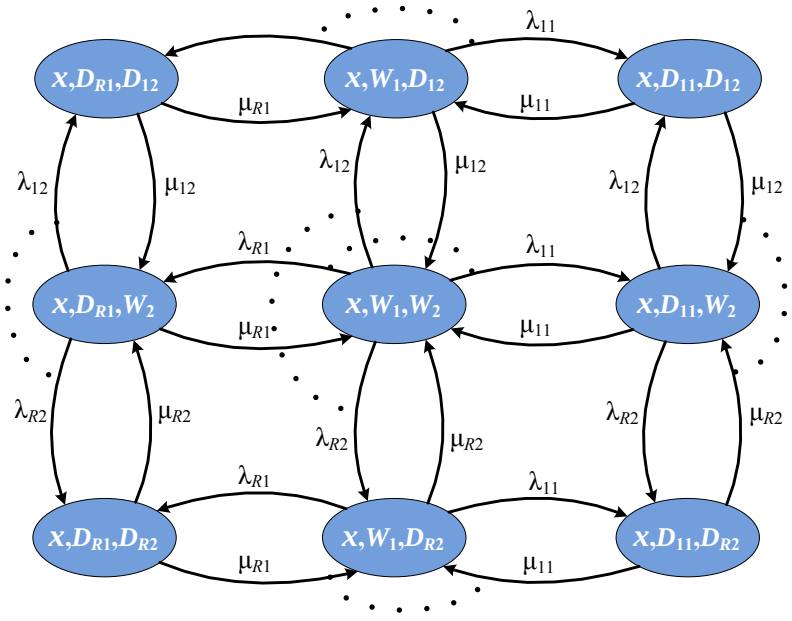

Figure 10. State transition diagram when $x \in]0, N_j[$ for case (R, R).

The number of internal states is $(R+1)^2$. There are also $(R+1)^2$ possible states of the form $(N_j, \alpha_j, \alpha_{j+1})$ and $(R+1)^2$ possible states of the form $(0, \alpha_j, \alpha_{j+1})$. Tables 3 and 4 characterize the reachable high and low boundary states, respectively. In these Tables, the indices i and j refer to the number of failure modes for machines M_1 and M_2, respectively. Therefore, we have $i = 1,\ldots, R$ and $j = 1,\ldots, R$.

Table 3. Combinations of states when the buffer is full for case (R, R).

State	Justification
(N_1, D_{i1}, W_2)	Unreachable: as M_2 is working and M_1 is down in failure mode i, the buffer will necessarily decrease.
(N_1, D_{i1}, D_{j2})	Unreachable: see remark 3 below.
$(N_1, \overline{W_1}, D_{j2})$	Reachable: when M_1 is working and M_2 is down in failure mode j, the buffer will become full; then M_1 becomes blocked.
(N_1, W_1, W_2)	Reachable: when M_2 is repaired from state $(N_1, \overline{W_1}, D_{j2})$, this state is reached knowing that $U_1 = U_2$.

Remark 3.

State (N_1, D_{i1}, D_{j2}) is unreachable because the only way to reach it is either to transit:

- from state (N_1, D_{i1}, W_2) which is unreachable; or
- from state $(N_1, \overline{W_1}, D_{j2})$; but since M_1 is blocked, it cannot fail and such a transition is not possible.

Table 4. Combinations of states when the buffer is empty for case (*R*, *R*).

State	Justification
$\left(0, D_{i1}, \underline{W_2}\right)$	Reachable: when M_1 is down in failure mode i and M_2 is working, the buffer will be empty, then M_2 becomes starved.
$(0, W_1, W_2)$	Reachable: when M_1 is repaired from state $\left(0, D_{i1}, \underline{W_2}\right)$, this state is reached knowing that $U_1 = U_2$.
$\left(0, D_{i1}, D_{j2}\right)$	Unreachable: see remark 4 below.
$\left(0, W_1, D_{j2}\right)$	Unreachable: when M_1 is working and M_2 is down in failure mode j, the buffer cannot be empty.

Remark 4.

State $\left(0, D_{i1}, D_{j2}\right)$ is unreachable because the only way to reach it is either to transit:

- from state $\left(0, W_1, D_{j2}\right)$ which is unreachable; or
- from state $\left(0, D_{i1}, \underline{W_2}\right)$; but since M_2 is starved, it cannot fail and such a transition is impossible.

Finally, by defining the remaining feasible transitions, we obtain the dipole Markov chain sketched in Figure 11.

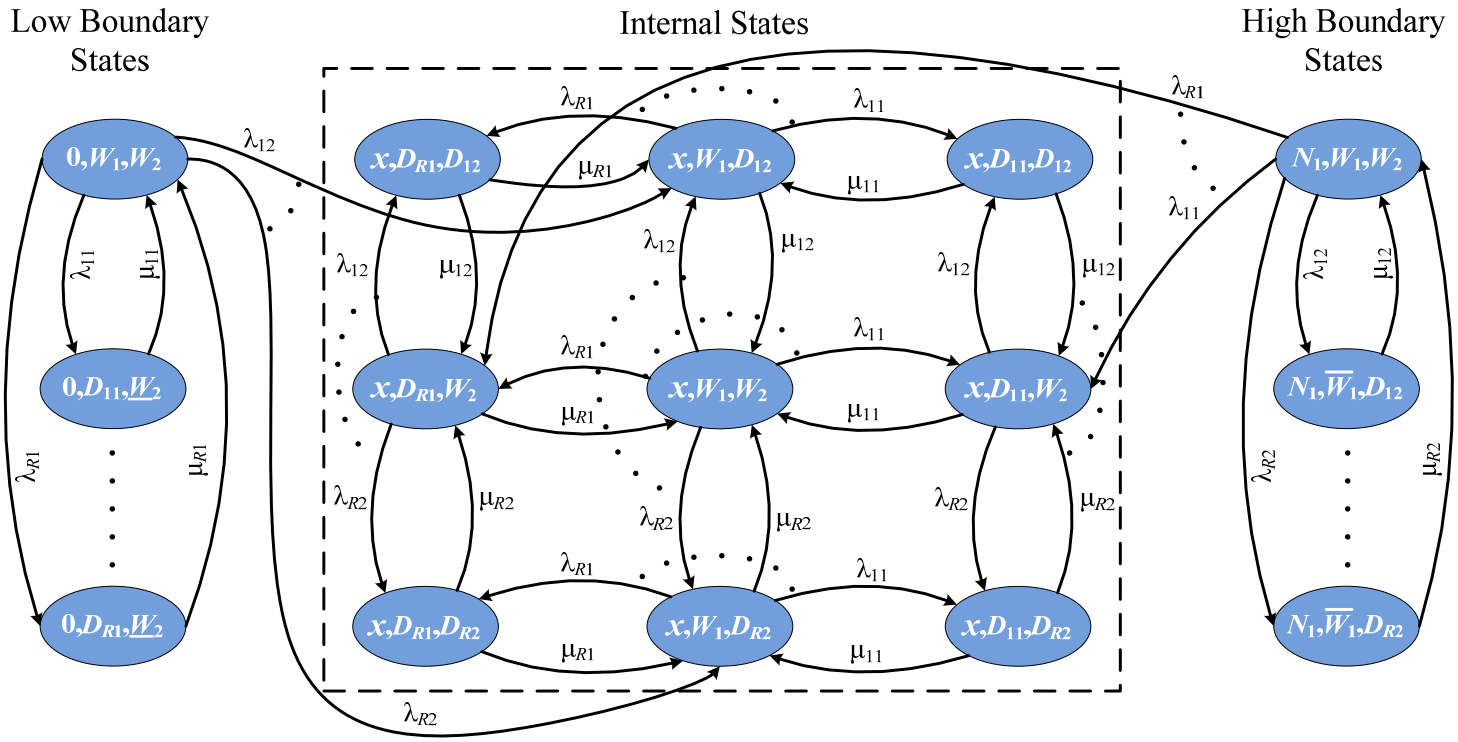

Figure 11. The dipole Markov chain for case (R, R).

4.2. Evaluation of the state probabilities

Once the Markov chain is defined, the state probabilities are evaluated by solving the corresponding Chapman-Kolmogorov (CK) equations, where a balance equation is written for each state. For example, the CK equation for state (x, W_1, W_2) is:

$$-\left(\sum_{i=1}^{R}\lambda_{i1}+\sum_{j=1}^{R}\lambda_{j2}\right)p(x,W_1,W_2)+\sum_{i=1}^{R}\mu_{i1}p(x,D_{i1},W_2)+\sum_{j=1}^{R}\mu_{j2}p(x,W_1,D_{j2})=0, \quad (1)$$

where $p(E)$ represents the probability for the system to be in state E.

Even if we have many states, it is possible to write CK equations in a compact form by identifying states with similar transitions. In fact, with $i = 1,\ldots, R$ and $j = 1,\ldots, R$, we can write:

- For states (x, D_{11}, W_2), (x, D_{21}, W_2), ..., (x, D_{R1}, W_2), we have:

$$-\left(\mu_{i1}+\sum_{j=1}^{R}\lambda_{j2}\right)p(x, D_{i1}, W_2)+\lambda_{i1}p(x, W_1, W_2)+\sum_{j=1}^{R}\mu_{j2}p\left(x, D_{i1}, D_{j2}\right)+\lambda_{i1}p(N_1, W_1, W_2)=0. \quad (2)$$

- For states (x, W_1, D_{12}), (x, W_1, D_{22}), ..., (x, W_1, D_{R2}), we have:

$$-\left(\mu_{j2}+\sum_{i=1}^{R}\lambda_{i1}\right)p\left(x, W_1, D_{j2}\right)+\sum_{i=1}^{R}\mu_{i1}p\left(x, D_{i1}, D_{j2}\right)+\lambda_{j2}p(x, W_1, W_2)+\lambda_{j2}p(0, W_1, W_2)=0. \quad (3)$$

- For states (x, D_{11}, D_{12}), (x, D_{11}, D_{22}), (x, D_{21}, D_{12}), (x, D_{21}, D_{22}), ..., (x, D_{R1}, D_{R2}), we have:

$$-\left(\mu_{i1}+\mu_{j2}\right)p\left(x, D_{i1}, D_{j2}\right)+\lambda_{j2}p(x, D_{i1}, W_2)+\lambda_{i1}p\left(x, W_1, D_{j2}\right)=0. \quad (4)$$

- For state (N_1, W_1, W_2), we have:

$$-\left(\sum_{i=1}^{R}\lambda_{i1}+\sum_{j=1}^{R}\lambda_{j2}\right)p(N_1, W_1, W_2)+\sum_{j=1}^{R}\mu_{j2}p\left(N_1, \overline{W_1}, D_{j2}\right)=0. \quad (5)$$

- For states $(N_1, \overline{W_1}, D_{12})$, $(N_1, \overline{W_1}, D_{22})$, ..., $(N_1, \overline{W_1}, D_{R2})$, we have:

$$-\lambda_{j2}p(N_1, W_1, W_2)+\mu_{j2}p\left(N_1, \overline{W_1}, D_{j2}\right)=0. \quad (6)$$

- For state $(0, W_1, W_2)$, we have:

$$-\left(\sum_{i=1}^{R}\lambda_{i1}+\sum_{j=1}^{R}\lambda_{j2}\right)p(0, W_1, W_2)+\sum_{i=1}^{R}\mu_{i1}p(0, D_{i1}, \underline{W_2})=0. \quad (7)$$

- For states $(0, D_{11}, \underline{W_2})$, $(0, D_{21}, \underline{W_2})$, ..., $(0, D_{R1}, \underline{W_2})$, we have:

$$-\lambda_{i1}p(0, W_1, W_2)+\mu_{i1}p\left(0, D_{i1}, \underline{W_2}\right)=0. \quad (8)$$

Furthermore, we have for $\alpha_1 \in \{W_1, D_{11}, \ldots, D_{R1}\}$ and $\alpha_2 \in \{W_2, D_{12}, \ldots, D_{R2}\}$:

$$\sum_{\alpha_1}\sum_{\alpha_2}\left[\int_0^{N_1}p(x, \alpha_1, \alpha_2)dx+p(0, \alpha_1, \alpha_2)+p(N_1, \alpha_1, \alpha_2)\right]=1. \quad (9)$$

Following the same procedure as in (Dubois and Forestier, 1982; Levantesi *et al.*, 2002), we obtain the state probabilities by solving the above CK equations (see (Belmansour, 2007) for more details).

4.3. Classification of states and equivalent machine

4.3.1. Each machine has two failure modes

In this step, the dipole MC of Figure 8 is approximated by an equivalent machine M_{eq} with three states (see Figure 12).

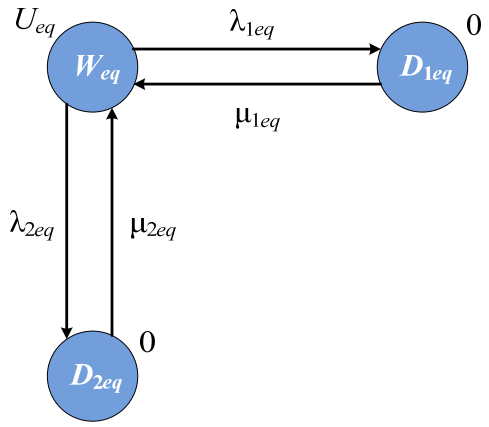

Figure 12. Equivalent machine Markov chain for case (2, 2).

To define the states and the parameters of M_{eq}, the states of the MC in Figure 8 are classified to form three macro-states as follows:

- **Macro-state W_{eq}:** The dipole will produce parts at the output if M_2 is in its working state (W_2). That is, seen from the downstream, the dipole is working for all states where M_2 is working. Therefore, the macro-state W_{eq} is composed of states (x, W_1, W_2), $(0, W_1, W_2)$, (N_1, W_1, W_2), (x, D_{11}, W_2) and (x, D_{21}, W_2).
- **Macro-state D_{1eq}:** We consider that the dipole is down in failure mode 1 when:
  - M_2 is down in failure mode 1 (states (x, W_1, D_{12}), (x, D_{11}, D_{12}), (x, D_{21}, D_{12}), $(N_1, \overline{W_1}, D_{12})$); or
  - M_2 is starved due to M_1 failure mode 1 (state $(0, D_{11}, \underline{W_2})$).

- **Macro-state D_{2eq}:** We consider that the dipole is down in failure mode 2 when:
  - M_2 is down in failure mode 2 (states (x, W_1, D_{22}), (x, D_{11}, D_{22}), (x, D_{21}, D_{22}), $(N_1, \overline{W_1}, D_{22})$); or
  - M_2 is starved due to M_1 failure mode 2 (state $(0, D_{21}, \underline{W_2})$).

Considering these three macro-states, the dipole MC of Figure 8 can be represented by Figure 13 where only transitions between macro-states are kept. Furthermore, in this figure, we introduce the transitions τ_1 and τ_2 to take into account the stock behaviour as follows:

- in state (x, D_{11}, W_2) it is possible to reach state $(0, D_{11}, \underline{W_2})$; and
- in state (x, D_{21}, W_2) it is possible to reach state $(0, D_{21}, \underline{W_2})$.

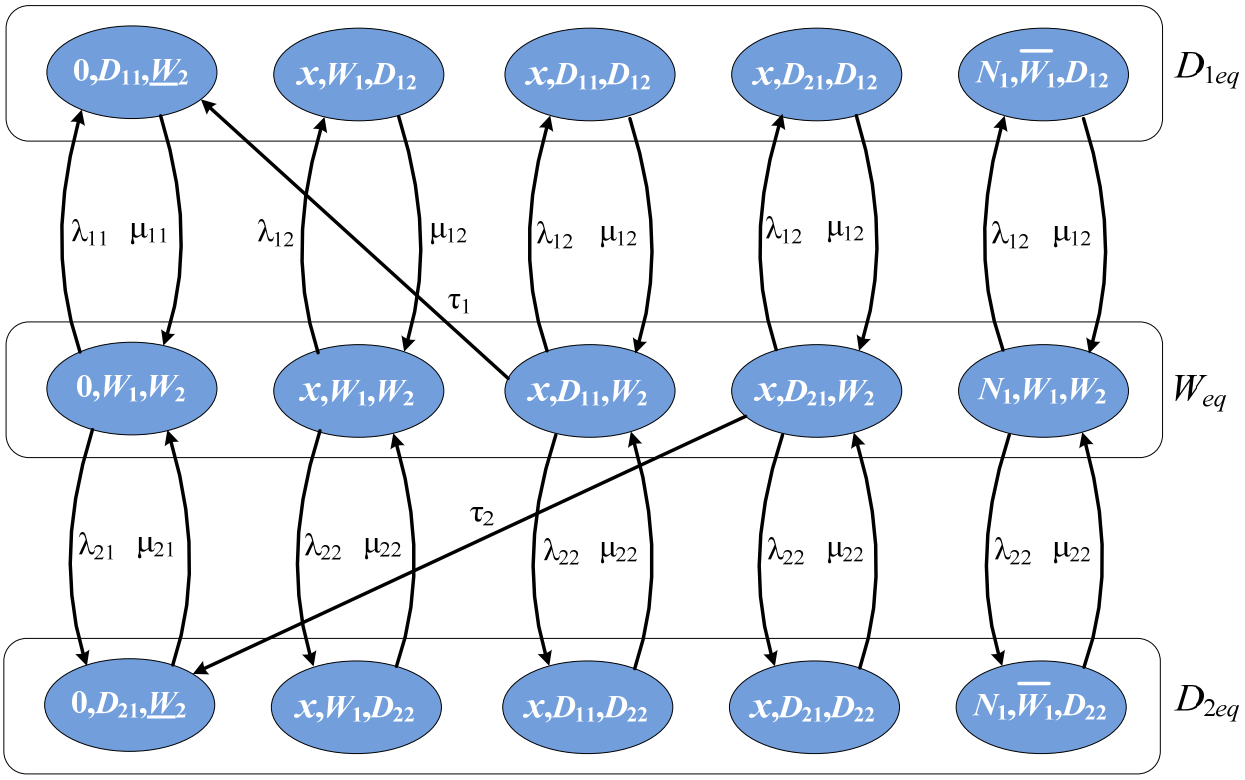

Figure 13. Macro-states and transitions for M_{eq} (case (2, 2)).

4.3.2. Each machine has *R* failure modes

Similarly, for case (R, R), the dipole MC in Figure 11 is approximated by the equivalent machine (M_{eq}) in Figure 14. The macro-states and transitions for M_{eq} in case (R, R) are given by Figure 15. In the next step, the parameters of M_{eq} are evaluated.

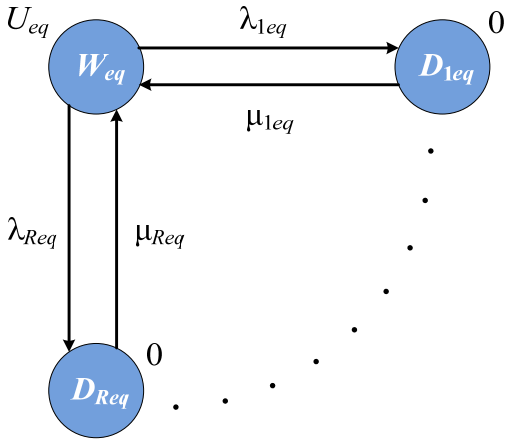

Figure 14. Equivalent machine Markov chain for case (R, R).

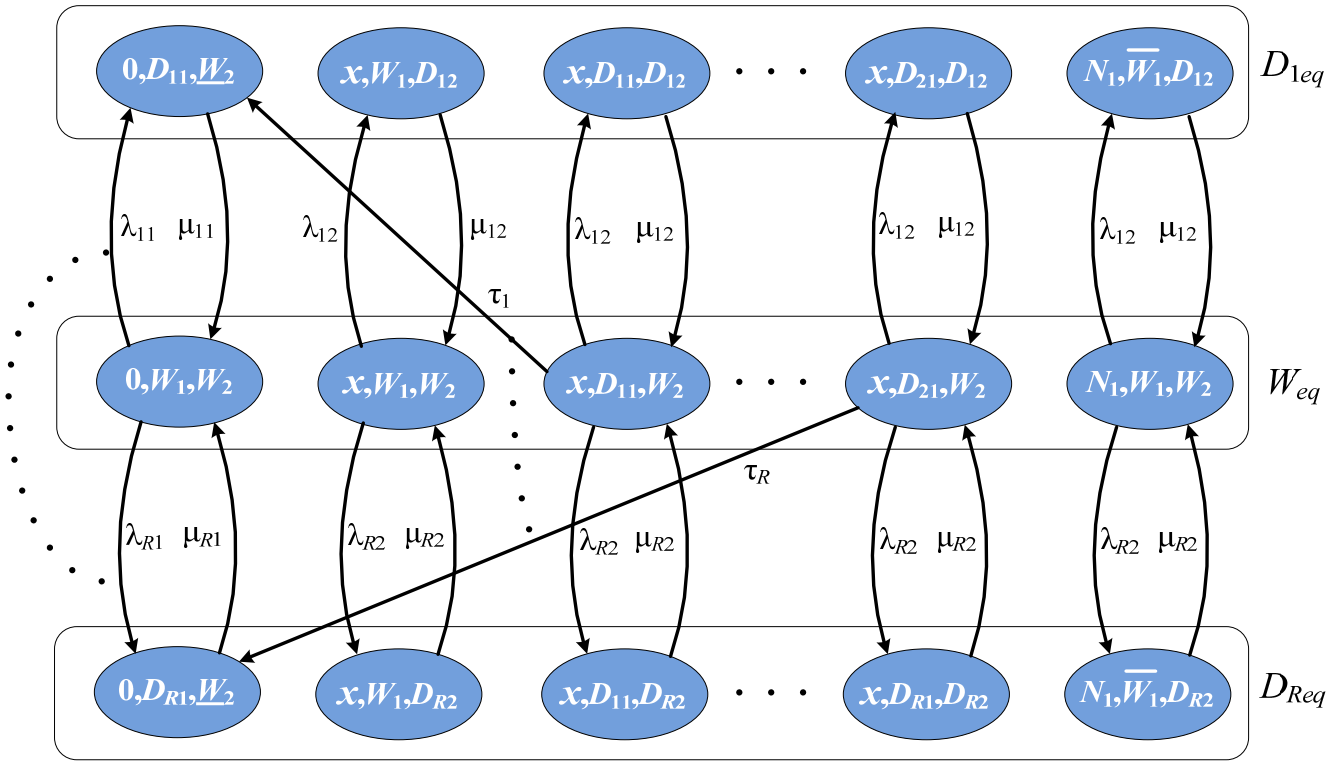

Figure 15. Macro-states and transitions for M_{eq} (case (R, R)).

4.4. Parameters evaluation

4.4.1. Each machine has two failure modes

Once the macro-states and the transitions have been defined, we can now evaluate the parameters of M_{eq} by means of weighted averages of the transition rates. We obtain:

$$\lambda_{1eq}=\frac{\lambda_{11}p(0, W_1, W_2)+\lambda_{12}p(x, W_1, W_2)+(\lambda_{12}+\tau_1)p(x, D_{11}, W_2)+\lambda_{12}p(x, D_{21}, W_2)}{p(0, W_1, W_2)+p(x, W_1, W_2)+p(x, D_{11}, W_2)+p(x, D_{21}, W_2)+p(N_1, W_1, W_2)}$$

$$+\frac{\lambda_{12}p(N_1, W_1, W_2)}{p(0, W_1, W_2)+p(x, W_1, W_2)+p(x, D_{11}, W_2)+p(x, D_{21}, W_2)+p(N_1, W_1, W_2)}. \quad (10)$$

$$\mu_{1eq}=\frac{\mu_{11}p\left(0, D_{11}, \underline{W_2}\right)+\mu_{12}p(x, W_1, D_{12})+\mu_{12}p(x, D_{11}, D_{12})+\mu_{12}p(x, D_{21}, D_{12})}{p\left(0, D_{11}, \underline{W_2}\right)+p(x, W_1, D_{12})+p(x, D_{11}, D_{12})+p(x, D_{21}, D_{12})+p\left(N_1, \overline{W_1}, D_{12}\right)}$$

$$+\frac{\mu_{12}p\left(N_1, \overline{W_1}, D_{12}\right)}{p\left(0, D_{11}, \underline{W_2}\right)+p(x, W_1, D_{12})+p(x, D_{11}, D_{12})+p(x, D_{21}, D_{12})+p\left(N_1, \overline{W_1}, D_{12}\right)}. \quad (11)$$

$$\lambda_{2eq}=\frac{\lambda_{21}p(0, W_1, W_2)+\lambda_{22}p(x, W_1, W_2)+\lambda_{22}p(x, D_{11}, W_2)+(\lambda_{22}+\tau_2)p(x, D_{21}, W_2)}{p(0, W_1, W_2)+p(x, W_1, W_2)+p(x, D_{11}, W_2)+p(x, D_{21}, W_2)+p(N_1, W_1, W_2)}$$

$$+\frac{\lambda_{22}p(N_1, W_1, W_2)}{p(0, W_1, W_2)+p(x, W_1, W_2)+p(x, D_{11}, W_2)+p(x, D_{21}, W_2)+p(N_1, W_1, W_2)}. \quad (12)$$

$$\mu_{2eq}=\frac{\mu_{21}p\left(0, D_{21}, \underline{W_2}\right)+\mu_{22}p(x, W_1, D_{22})+\mu_{22}p(x, D_{11}, D_{22})+\mu_{22}p(x, D_{21}, D_{22})}{p\left(0, D_{21}, \underline{W_2}\right)+p(x, W_1, D_{22})+p(x, D_{11}, D_{22})+p(x, D_{21}, D_{22})+p\left(N_1, \overline{W_1}, D_{22}\right)}$$

$$+\frac{\mu_{22}p\left(N_1, \overline{W_1}, D_{22}\right)}{p\left(0, D_{21}, \underline{W_2}\right)+p(x, W_1, D_{22})+p(x, D_{11}, D_{22})+p(x, D_{21}, D_{22})+p\left(N_1, \overline{W_1}, D_{22}\right)}. \quad (13)$$

In these equations, we remark that the only remaining unknowns are τ_1 and τ_2. These parameters are evaluated by writing CK equation for states $\left(0, D_{11}, \underline{W_2}\right)$ and $\left(0, D_{21}, \underline{W_2}\right)$:

$$\tau_1 p(x, D_{11}, W_2)+\lambda_{11}p(0, W_1, W_2)=\mu_{11}p\left(0, D_{11}, \underline{W_2}\right), \quad (14)$$

$$\tau_2 p(x, D_{21}, W_2) + \lambda_{21} p(0, W_1, W_2) = \mu_{21} p\left(0, D_{21}, \underline{W_2}\right). \tag{15}$$

From equations (14) and (15), we obtain:

$$\tau_1 = \frac{\mu_{11} p\left(0, D_{11}, \underline{W_2}\right) - \lambda_{11} p(0, W_1, W_2)}{p(x, D_{11}, W_2)}, \tag{16}$$

and

$$\tau_2 = \frac{\mu_{21} p\left(0, D_{21}, \underline{W_2}\right) - \lambda_{21} p(0, W_1, W_2)}{p(x, D_{21}, W_2)}. \tag{17}$$

4.4.2. Each machine has *R* failure modes

Similarly, we obtain:

$$\lambda_{1eq} = \frac{\lambda_{11} p(0, W_1, W_2) + \lambda_{12} p(x, W_1, W_2) + (\lambda_{12} + \tau_1) p(x, D_{11}, W_2)}{p(0,W_1,W_2) + p(x,W_1,W_2) + p(x, D_{11},W_2) + p(x, D_{21},W_2) + \ldots + p(x, D_{R1}, W_2) + p(N_1,W_1,W_2)}$$

$$+ \frac{\lambda_{12} p(x, D_{21}, W_2) + \ldots + \lambda_{12} p(x, D_{R1}, W_2) + \lambda_{12} p(N_1,W_1,W_2)}{p(0,W_1,W_2) + p(x,W_1,W_2) + p(x, D_{11},W_2) + p(x, D_{21},W_2) + \ldots + p(x, D_{R1}, W_2) + p(N_1,W_1,W_2)}. \tag{18}$$

$$\mu_{1eq} = \frac{\mu_{11} p\left(0, D_{11}, \underline{W_2}\right) + \mu_{12} p(x, W_1, D_{12}) + \mu_{12} p(x, D_{11}, D_{12})}{p\left(0, D_{11}, \underline{W_2}\right) + p(x, W_1, D_{12}) + p(x, D_{11}, D_{12}) + p(x, D_{21}, D_{12}) + \ldots + p(x, D_{R1}, D_{12}) + p\left(N_1, \overline{W_1}, D_{12}\right)}$$

$$+ \frac{\mu_{12} p(x, D_{21}, D_{12}) + \ldots + \mu_{12} p(x, D_{R1}, D_{12}) + \mu_{12} p\left(N_1, \overline{W_1}, D_{12}\right)}{p\left(0, D_{11}, \underline{W_2}\right) + p(x, W_1, D_{12}) + p(x, D_{11}, D_{12}) + p(x, D_{21}, D_{12}) + \ldots + p(x, D_{R1}, D_{12}) + p(N_1, \overline{W_1}, D_{12})}. \tag{19}$$

and so on, up to:

$$\lambda_{Req} = \frac{\lambda_{R1} p(0,W_1,W_2) + \lambda_{R2} p(x,W_1,W_2) + \lambda_{R2} p(x, D_{11},W_2) + \ldots + (\lambda_{R2} + \tau_R) p(x, D_{R1},W_2) + \lambda_{R2} p(N_1,W_1,W_2)}{p(0,W_1,W_2) + p(x,W_1,W_2) + p(x, D_{11},W_2) + \ldots + p(x, D_{R1},W_2) + p(N_1,W_1,W_2)}. \tag{20}$$

$$\mu_{Req} = \frac{\mu_{R1} p\left(0, D_{R1}, \underline{W_2}\right) + \mu_{R2} p(x, W_1, D_{R2}) + \mu_{R2} p(x, D_{11}, D_{R2}) + \ldots + \mu_{R2} p(x, D_{R1}, D_{R2}) + \mu_{R2} p\left(N_1, \overline{W_1}, D_{R2}\right)}{p\left(0, D_{R1}, \underline{W_2}\right) + p(x, W_1, D_{R2}) + p(x, D_{11}, D_{R2}) + \ldots + p(x, D_{R1}, D_{R2}) + p\left(N_1, \overline{W_1}, D_{R2}\right)}. \tag{21}$$

In these equations, the only remaining unknowns are $\tau_1, \tau_2, \ldots, \tau_R$ that are again evaluated by writing for $i = 1, \ldots, R$:

$$\tau_i p(x, D_{i1}, W_2) + \lambda_{i1} p(0, W_1, W_2) = \mu_{i1} p\left(0, D_{i1}, \underline{W_2}\right). \quad (22)$$

From equation (22), we obtain:

$$\tau_i = \frac{\mu_{i1} p\left(0, D_{i1}, \underline{W_2}\right) - \lambda_{i1} p(0, W_1, W_2)}{p(x, D_{i1}, W_2)}. \quad (23)$$

4.5. Estimation of the dipole production rate $\overline{U}$

The production rate $\overline{U}$ is the sum of two quantities $\overline{U_1}$ and $\overline{U_2}$. The value of $\overline{U_1}$ is obtained by multiplying the nominal production rate of the equivalent machine M_{eq} by its availability:

$$\overline{U_1} = U \times \frac{1}{1 + \frac{\lambda_{1eq}}{\mu_{1eq}} + \ldots + \frac{\lambda_{Req}}{\mu_{Req}}}. \quad (24)$$

Notice that equation (24) does not take into account the environment of the aggregated dipole. However, to estimate the production rate of the dipole, we have to take into account its environment as it is a part of the whole production line. The notions of the dipole environment and that of the supplementary production were first introduced in (Terracol and David, 1987(a), (b)). To illustrate these notions, let us consider for example the first aggregation step in Figure 2. The behaviour of M_{34} (the equivalent machine of (M_3, B_3, M_4)) depends on B_2 and M_2. By using equation (24) it is implicitly assumed that when B_2 is empty and M_2 is down, M_{34} is starved. Even if M_3 is starved, M_4 can continue producing parts while B_3 is not empty. This kind of situation leads to a supplementary production quantity. Then, an additional production rate ($\overline{U_2}$) has to be added to $\overline{U_1}$ to obtain a more accurate estimation of the dipole production rate $\overline{U} = \overline{U_1} + \overline{U_2}$.

The production rate $\overline{U_2}$ is given by the product of the following two quantities (Terracol and David, 1987(a), (b)): (*i*) the production rate I injected by M_4 when B_2 is empty and M_2 is down; and (*ii*) the probability p_d that this injected production is effectively reflected on the production line. That is, $\overline{U_2} = I \times p_d$. The term I is evaluated by using an approach similar to that proposed in (Terracol and David, 1987(a), (b)) for one failure mode: see (Belmansour and Nourelfath, 2008) for more details. The value of p_d corresponds to the probability that B_3 is not empty, and it is given by:

$$p_d = \frac{\sum_{j=1}^{R} p(x, W_1, D_{j2}) \times \tau_j}{\sum_{i=1}^{R} p(x, D_{i1}, W_2) \times \tau_i + \sum_{j=1}^{R} p(x, W_1, D_{j2}) \times \tau_j}. \quad (25)$$

4.5.1. Updating the parameters of M_{eq}

The parameters λ_{ieq} and μ_{ieq} $(i = 1,\ldots, R)$ have been evaluated in subsection 4.4.2 without taking into account the supplementary production rate $\overline{U_2}$. The machine M_{eq} can be defined as a single failure mode machine with a parameter $\lambda_{eq} = \sum_{i=1}^{R} \lambda_{ieq}$. In order to preserve the same availability of M_{eq}, the parameter μ_{eq} is given by:

$$\frac{1}{\mu_{eq}} = \sum_{i=1}^{R} \left(\frac{\lambda_{ieq}}{\sum_{i=1}^{R} \lambda_{ieq}} \times \frac{1}{\mu_{ieq}} \right). \quad (26)$$

The new production introduced by $\overline{U_2}$ can be interpreted as a reduction in the failure rate of M_{eq}. Therefore, this failure rate is updated as λ_{eq}^* by using:

$$\overline{U} = U \times \frac{\mu_{eq}}{\lambda_{eq}^* + \mu_{eq}}. \quad (27)$$

Then,

$$\lambda_{eq}^* = \frac{U \times \mu_{eq}}{\overline{U}} - \mu_{eq}. \quad (28)$$

By considering $\lambda_{eq}^* = \sum_{i=1}^{R} \lambda_{ieq}^*$, we can write:

$$\lambda_{eq}^* = v_i \times \lambda_{ieq}^* \quad \text{for } i = 1, 2,\ldots, R, \quad (29)$$

$$\text{with } \sum_{i=1}^{R} v_i = 1. \quad (30)$$

Then, we put $\lambda_{ieq} = v_i \times \lambda_{eq}$ and we determine λ_{ieq}^* as follows:

$$\lambda^*_{ieq} = \frac{\lambda_{ieq}}{\lambda_{eq}} \times \lambda^*_{eq} \quad \text{for } i = 1, 2, \ldots, R. \tag{31}$$

The final parameters of the machine M_{eq} are λ^*_{ieq}, μ_{ieq} and U, and its production rate is:

$$\overline{U} = \overline{U_1} + \overline{U_2} = U \times \frac{1}{1 + \sum_{i=1}^{R} \frac{\lambda^*_{ieq}}{\mu_{ieq}}}. \tag{32}$$

5. Numerical experiments

The simulation models of the tandem lines with machines having multiple failure modes were developed by using the commercial package *ProModel*. Many examples were considered where all failure and repair rates were assumed to have an exponential distribution. Each model was run for a 500 time units warm-up period to reach its steady state. The production rate for the next 6,000 time units was then collected. Each simulation was run ten times for each system. The second step of our study was to apply the proposed aggregation method on the considered examples, and then to compare the obtained results with those obtained by simulating the original systems. The percentage error in production rate ($\overline{U}$) is calculated by:

$$Error1\ \% = \frac{\overline{U}_{(A)} - \overline{U}_{(S)}}{\overline{U}_{(S)}} \times 100, \tag{33}$$

where $\overline{U}_{(A)}$ and $\overline{U}_{(S)}$ are production rates estimated from the analytical aggregation method and the simulation, respectively. Simulation models and approximate analytical solution were compared for six examples with parameters data given in appendix A (Tables A.1 to A.6). Each machine in these examples has two failure modes, and the length of the line varies from 5 to 15 machines.

Furthermore, to evaluate the accuracy level gained by using our aggregation method considering multiple failure modes instead of a classical aggregation method considering only one failure mode per machine (Terracol and David, 1987(a), (b)), we calculate:

$$Error2\ \% = \frac{U_{(A)} - \overline{U}_{(S)}}{\overline{U}_{(S)}} \times 100, \tag{34}$$

$$\text{and } \Delta\ \% = |Error2\ \% - Error1\%|, \tag{35}$$

where $\underline{U}_{(A)}$ is the production rate estimated from the aggregation method when each machine is transformed into a single failure mode machine. To illustrate this transformation, let us consider a machine with two failure modes characterized by $\lambda_1, \mu_1, \lambda_2$ and μ_2. This machine corresponds to a single failure mode machine with parameters λ and μ, such as:

$$\lambda = \lambda_1 + \lambda_2, \tag{36}$$

and both machines have the same availability. This means that:

$$\frac{1}{1+\frac{\lambda}{\mu}} = \frac{1}{1+\frac{\lambda_1}{\mu_1}+\frac{\lambda_2}{\mu_2}}. \tag{37}$$

From the above equation, we obtain:

$$\frac{1}{\mu} = \left(\frac{\lambda_1}{\lambda_1+\lambda_2}\times\frac{1}{\mu_1}\right)+\left(\frac{\lambda_2}{\lambda_1+\lambda_2}\times\frac{1}{\mu_2}\right). \tag{38}$$

Tables B.1 to B.6 in appendix B presents, for each example, the parameters of corresponding single failure mode machines using equations (36) and (38).

Table 5 shows the comparison of the production rate from our analytical method and the simulation (*Error*1 *%*). The average absolute value of the percentage error in the production rate estimation is less than 4.5 *%* for all examples. This table also shows that the proposed aggregation method is more accurate than the existing one for all examples (since $|Error1\ \%| < |Error2\ \%|$). Furthermore, the value of $\Delta\ \%$ shows that the accuracy level gained by our method varies from 1.94 *%* to 3.98 *%*.

Table 5. Comparison results.

	Simulation Results	Proposed aggregation method	Existing aggregation method	Error1 %	Error2 %	Δ%
Example 1	0.56508	0.54350	0.52676	- 6.78	- 3.81	2.97
Example 2	0.58478	0.56116	0.53793	- 8.01	- 4.03	3.98
Example 3	0.82297	0.82484	0.80877	- 1.72	0.22	1.94
Example 4	0.52239	0.49911	0.48548	- 7.06	- 4.45	2.61
Example 5	2.67247	2.66626	2.59733	- 2.81	- 0.23	2.58
Example 6	0.60723	0.58498	0.56644	- 6.71	- 3.66	3.05

By considering the case of a dipole, we now show that the accuracy improvement level brought by our aggregation method is higher when the availability parameters of the various failure modes differ significantly. We consider dipoles in which each machine has two failure modes. Table 6 presents the parameters data for the initial dipole.

Table 6. Initial parameters of the machines.

Machine k	U	λ_{1k}	μ_{1k}	λ_{2k}	μ_{2k}	N_k
Machine 1	1.03	0.0022	0.0696	0.0178	0.2611	20
Machine 2	1.03	0.01	0.1494			

The availability and the failure rates of both machines (M_1 and M_2) are kept constant while the repair rates of the upstream machine (M_1) are varied. Figure 16 shows the graph of the average production rate $\overline{U}$ versus μ_{11}. In order to preserve the same availability for M_1, as μ_{11} increases, μ_{21} must decrease. In the right scale of the graph of Figure 16, the percentage difference between the two methods is given by:

$$Error\ \% = \frac{\underline{U}_{(A)} - \overline{U}_{(A)}}{\overline{U}_{(A)}} \times 100. \tag{39}$$

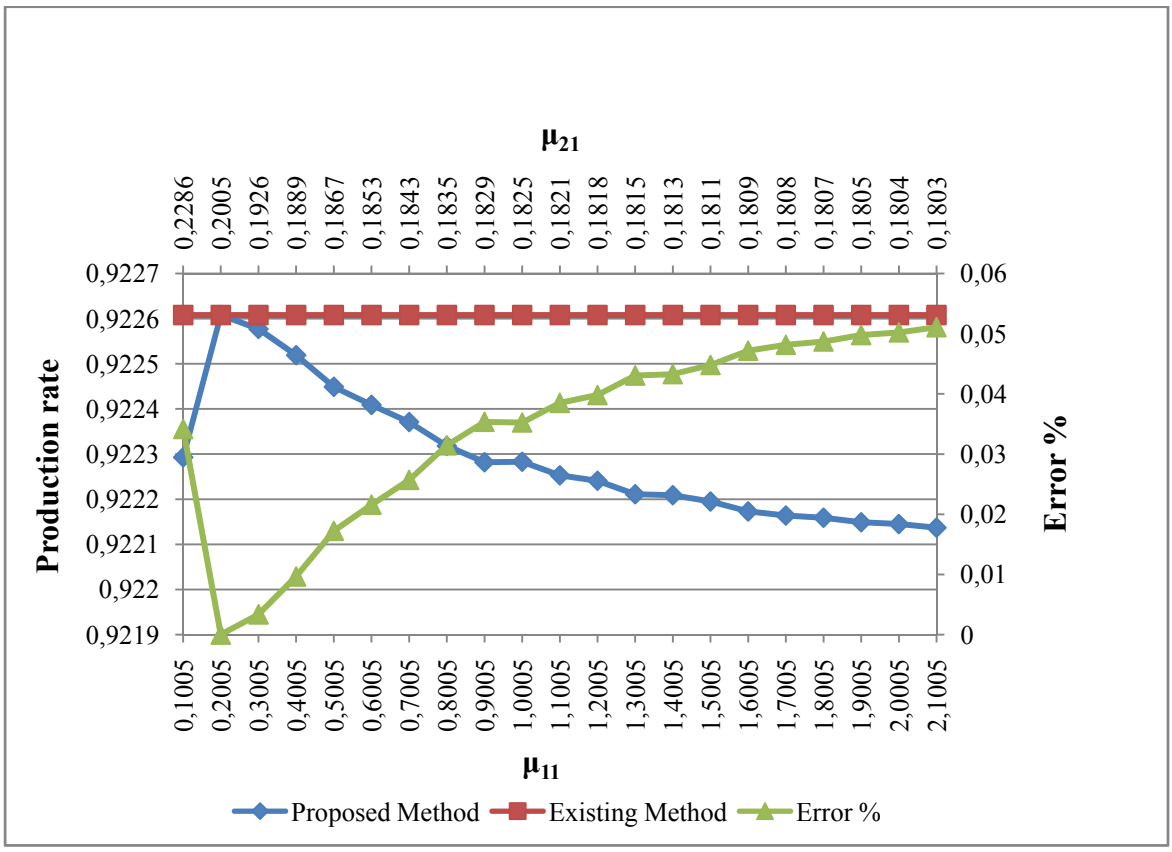

Figure 16. Average production rate as a function of μ_{11}.

From Figure 16, it can be observed that when $\mu = \mu_{11} = \mu_{21} = 0.2005$ both the existing and the proposed model give the same results: as the two failure modes have the same repair rate, there is no need to distinguish among them and the average failure does not introduce any error. In all the other cases, the existing method tends to overestimate the average production rate. This can be explained by the fact that when $\mu_{11} \neq \mu_{21}$ (although the machine availability is kept constant), one of the two modes has a repair probability lower than μ which means a longer MTTR and a higher probability of starvation for the downstream machine. We remark that the error increases when the availability parameters of the various failure modes differ significantly, meaning that the accuracy improvement level brought by our aggregation method is higher.

6. Conclusions

An aggregation method for the performance evaluation of a tandem production line, with machines having multiple failure modes, has been developed. The main characteristic of the proposed method is its ability to evaluate quickly the production rate of a line in which machines can have multiple failure modes. Indeed, this is more realistic since machines can be affected by a wide range of failures, which occur with different frequencies and require different amount of time to be repaired. Simulation experiments and numerical results have shown the accuracy of the proposed aggregation method. By distinguishing among different failure modes for each machine, we obtain a more accurate evaluation of the performance measure, especially when the reliability parameters of the failure modes have significantly different orders of magnitude. To qualify this improvement, we made a comparison with the aggregation method proposed in (Terracol and David, 1987(a), (b)) that considers one failure mode per machine.

We are currently working on the extension of the method to the analysis of asynchronous tandem production lines, with machines having a number of failure modes that may differ from one machine to another.

Acknowledgements

The authors would like to thank the Natural Sciences and Engineering Research Council of Canada (NSERC) for financial support.

References

Belmansour, A.T., 2007. *Évaluation du taux de production d'une ligne avec stocks intermédiaires et machines à deux modes de défaillances par la technique d'agrégation*. Mémoire de maîtrise (M.Sc. Thesis), Université du Québec en Abitibi-Témiscamingue, Quebec, Canada. In French.

Belmansour, A.T., & Nourelfath M., 2008. Taux de production d'une ligne avec stocks tampons et machines à deux modes de défaillances. *7^{e} conférence internationale de modélisation et simulation MOSIM'08*, 3, 1871-1880. In French.

Dallery, Y., David, R., & Xie, X., 1989. Approximate analysis of transfer lines with unreliable machines and finite buffers. *IEEE Transactions on Automatic Control,* 34 (9), 943-953.

Dallery, Y., & Gershwin, S.B., 1992. Manufacturing flow line system: A review of models and analytical results. *Queuing systems theory and applications*, (Special Issue on Queuing Model of Manufacturing System), 12 (1-2), 3-94.

De Koster, M.B.M., 1987. Estimation of line efficiency by aggregation. *International Journal of Production Research*, 25 (4), 615-626.

Dubois, D., & Forestier, J.P., 1982. Production et en-cours moyens d'un ensemble de deux machines séparées par une zone de stockage. *RAIRO Automatique*, 16 (2), 105-132.

Gershwin, S.B., 1987. An efficient decomposition method for the approximate evaluation of tandem queues with finite storage space and blocking. *Operations Research*, 35 (2), 291-305.

Gershwin, S.B., 1994. *Manufacturing systems engineering*. Upper Saddle River, NJ: Prentice Hall.

Hopcroft, J.E., & Ullman, J.D., 1979. *Introduction to automata theory, languages, and computation*. Addison-Wesley series in computer science.

Levantesi, R., Matta, A., & Tolio, T., 2002. Performance evaluation of production lines with random processing times, multiple failure modes and finite buffer capacity. Part I: the building block. *Analysis and Modeling of manufacturing systems. International Series in Operations Research & Management Science*, 60, Gershwin, S.B.; Dallery, Y.; Papadopoulos, C.T.; Smith, J.M. (Eds.) Springer. 181-200.

Levantesi, R., Matta, A., & Tolio, T., 2003. Performance evaluation of continuous production lines with machines having different processing times and multiple failure modes. *Performance Evaluation*, 51 (2-4), 247-268.

Li, J., 2005. Overlapping decomposition: A system-theoretic method for modeling and analysis of complex manufacturing systems. *IEEE Transactions on Automation Science and Engineering*, 2 (1), 40-53.

Nahas, N., Aït-Kadi, D., & Nourelfath, M., 2006. A new approach for buffer allocation in unreliable production lines. *International Journal of Production Economics*, 103 (2), 873-881.

Nahas, N., Nourelfath, M., & Aït-Kadi D., 2008. Selecting machines and buffers in unreliable series-parallel production lines. *International Journal of Production Research* (in press).

Nourelfath, M., Nahas, N., & Aït-Kadi D., 2005. Optimal design of unreliable series production lines with unreliable machines and finite buffers. *Journal of Quality in Maintenance Engineering*, 11 (2), 121-138.

Papadopoulos, H.T., & Heavey, C., 1996. Queuing theory in manufacturing systems analysis and design: A classification of models for production and transfer lines. *European Journal of Operational Research*, 92 (1), 1-27.

Sörensen, K., & Janssens, G.K., 2004. A Petri net model of a continuous flow transfer line with unreliable machines. *European Journal of Operational Research*, 152 (1), 248-262.

Terracol, C., & David, R., 1987 (a). Performances d'une ligne composée de machines et de stocks intermédiaires. *R.A.I.R.O APII*, 21 (3), 239-262.

Terracol, D., & David, R., 1987 (b). An aggregation method for performance evaluation of transfer lines with unreliable machines and finite buffers. *Proceedings of the IEEE International Conference on Robotics and Automation*, 1333-1338.

Tolio T., Matta A., & Gershwin S.B., 2002. Analysis of two-machine lines with multiple failure modes, *IIE Transactions*, 34 (1), 51-62.

Appendix A. Data for examples 1-6: two failure modes per machine

Table A.1. Example 1 data in the case of two failure modes per machine.

Machine k	U	λ_{1k}	μ_{1k}	λ_{2k}	μ_{2k}	N_k
Machine 1	1.200	0.0120	0.2200	0.0050	0.0400	55
Machine 2	1.200	0.0100	0.0400	0.0800	0.1500	40
Machine 3	1.200	0.1000	0.2000	0.0400	0.0900	40
Machine 4	1.200	0.0100	0.0870	0.1160	0.2971	55
Machine 5	1.200	0.1000	0.2500	0.0500	0.0800	

Table A.2. Example 2 data in the case of two failure modes per machine.

Machine k	U	λ_{1k}	μ_{1k}	λ_{2k}	μ_{2k}	N_k
Machine 1	1.4	0.0120	0.2200	0.0050	0.0400	20
Machine 2	1.4	0.0100	0.0400	0.0800	0.1500	20
Machine 3	1.4	0.1000	0.2000	0.0400	0.0900	20
Machine 4	1.4	0.0100	0.0870	0.1160	0.2971	20
Machine 5	1.4	0.1000	0.2500	0.0500	0.0800	

Table A.3. Example 3 data in the case of two failure modes per machine.

Machine k	U	λ_{1k}	μ_{1k}	λ_{2k}	μ_{2k}	N_k
Machine 1	1.030	0.0071	0.2323	0.0029	0.0422	20
Machine 2	1.030	0.0022	0.0696	0.0178	0.2611	20
Machine 3	1.030	0.0071	0.2024	0.0029	0.0910	20
Machine 4	1.030	0.0032	0.0698	0.0368	0.2383	20
Machine 5	1.030	0.0200	0.4273	0.0100	0.1366	

Table A.4. Example 4 data in the case of two failure modes per machine.

Machine k	U	λ_{1k}	μ_{1k}	λ_{2k}	μ_{2k}	N_k
Machine 1	1.100	0.0120	0.2200	0.0050	0.0400	55
Machine 2	1.100	0.0100	0.0400	0.0800	0.1500	40
Machine 3	1.100	0.1000	0.2000	0.0400	0.0900	40
Machine 4	1.100	0.0100	0.0870	0.1160	0.2971	55
Machine 5	1.100	0.1000	0.2500	0.0500	0.0800	50
Machine 6	1.100	0.0141	0.2323	0.0059	0.0422	50
Machine 7	1.100	0.0011	0.0348	0.0089	0.1306	65
Machine 8	1.100	0.0143	0.1350	0.0057	0.0607	55
Machine 9	1.100	0.0008	0.0349	0.0092	0.1192	35
Machine 10	1.100	0.0133	0.1709	0.0067	0.0546	

Table A.5. Example 5 data in the case of two failure modes per machine.

Machine k	U	λ_{1k}	μ_{1k}	λ_{2k}	μ_{2k}	N_k
Machine 1	3.5397	0.0190	0.3700	0.0079	0.0673	80
Machine 2	3.5397	0.0035	0.0679	0.0280	0.2546	65
Machine 3	3.5397	0.0346	0.2958	0.0138	0.1330	60
Machine 4	3.5397	0.0063	0.1354	0.0735	0.4621	70
Machine 5	3.5397	0.0140	0.3387	0.0070	0.1083	70
Machine 6	3.5397	0.0104	0.5064	0.0044	0.0921	70
Machine 7	3.5397	0.0019	0.0540	0.0153	0.2026	85
Machine 8	3.5397	0.0063	0.3462	0.0025	0.1557	80
Machine 9	3.5397	0.0009	0.0678	0.0104	0.2313	45
Machine 10	3.5397	0.0034	0.3184	0.0017	0.1018	

Table A.6. Example 6 data in the case of two failure modes per machine.

Machine k	U	λ_{1k}	μ_{1k}	λ_{2k}	μ_{2k}	N_k
Machine 1	1.300	0.0120	0.2200	0.0050	0.0400	55
Machine 2	1.300	0.0100	0.0400	0.0800	0.1500	40
Machine 3	1.300	0.1000	0.2000	0.0400	0.0900	40
Machine 4	1.300	0.0100	0.0870	0.1160	0.2971	55
Machine 5	1.300	0.1000	0.2500	0.0500	0.0800	50
Machine 6	1.300	0.0141	0.2323	0.0059	0.0422	50
Machine 7	1.300	0.0011	0.0348	0.0089	0.1306	65
Machine 8	1.300	0.0143	0.1350	0.0057	0.0607	55
Machine 9	1.300	0.0008	0.0349	0.0092	0.1192	35
Machine 10	1.300	0.0133	0.1709	0.0067	0.0546	40
Machine 11	1.300	0.0296	0.2323	0.0124	0.0422	55
Machine 12	1.300	0.0074	0.0696	0.0596	0.2611	40
Machine 13	1.300	0.0429	0.2024	0.0171	0.0910	50
Machine 14	1.300	0.0037	0.0698	0.0423	0.2383	55
Machine 15	1.300	0.0080	0.4273	0.0040	0.1366	

Appendix B. Data for examples 1-6: one failure mode per machine

Table B.1. Example 1 data in the case of one failure modes per machine.

Machine k	U	λ_k	μ_k	N_k
Machine 1	1.200	0.0170	0.0947	55
Machine 2	1.200	0.0900	0.1149	40
Machine 3	1.200	0.1400	0.1482	40
Machine 4	1.200	0.1260	0.2493	55
Machine 5	1.200	0.1500	0.1463	

Table B.2. Example 2 data in the case of one failure modes per machine.

Machine k	U	λ_k	μ_k	N_k
Machine 1	1.4	0.0170	0.0947	20
Machine 2	1.4	0.0900	0.1149	20
Machine 3	1.4	0.1400	0.1482	20
Machine 4	1.4	0.1260	0.2493	20
Machine 5	1.4	0.1500	0.1463	

Table B.3. Example 3 data in the case of one failure modes per machine.

Machine k	U	λ_k	μ_k	N_k
Machine 1	1.030	0.01	0.1007	20
Machine 2	1.030	0.02	0.2004	20
Machine 3	1.030	0.01	0.1494	20
Machine 4	1.030	0.04	0.1997	20
Machine 5	1.030	0.03	0.25	

Table B.4. Example 4 data in the case of one failure modes per machine.

Machine k	U	λ_k	μ_k	N_k
Machine 1	1.100	0.0170	0.0947	55
Machine 2	1.100	0.0900	0.1149	40
Machine 3	1.100	0.1400	0.1482	40
Machine 4	1.100	0.1260	0.2493	55
Machine 5	1.100	0.1500	0.1463	50
Machine 6	1.100	0.0200	0.1000	50
Machine 7	1.100	0.0100	0.1000	65
Machine 8	1.100	0.0200	0.1000	55
Machine 9	1.100	0.0100	0.1000	35
Machine 10	1.100	0.0200	0.1000	

Table B.5. Example 5 data in the case of one failure modes per machine.

Machine k	U	λ_k	μ_k	N_k
Machine 1	3.5397	0.0269	0.1593	80
Machine 2	3.5397	0.0315	0.195	65
Machine 3	3.5397	0.0484	0.2192	60
Machine 4	3.5397	0.0798	0.3878	70
Machine 5	3.5397	0.021	0.1982	70
Machine 6	3.5397	0.0148	0.218	70
Machine 7	3.5397	0.0172	0.1552	85
Machine 8	3.5397	0.0088	0.2565	80
Machine 9	3.5397	0.0113	0.1941	45
Machine 10	3.5397	0.0051	0.1863	

Table B.6. Example 6 data in the case of one failure modes per machine.

Machine k	U	λ_k	μ_k	N_k
Machine 1	1.300	0.0170	0.0947	55
Machine 2	1.300	0.0900	0.1149	40
Machine 3	1.300	0.1400	0.1482	40
Machine 4	1.300	0.1260	0.2493	55
Machine 5	1.300	0.1500	0.1463	50
Machine 6	1.300	0.0200	0.1000	50
Machine 7	1.300	0.0100	0.1000	65
Machine 8	1.300	0.0200	0.1000	55
Machine 9	1.300	0.0100	0.1000	35
Machine 10	1.300	0.0200	0.1000	40
Machine 11	1.300	0.0420	0.1000	55
Machine 12	1.300	0.0670	0.2000	40
Machine 13	1.300	0.0600	0.1500	50
Machine 14	1.300	0.0460	0.2000	55
Machine 15	1.300	0.0120	0.2500	